SYNTHESIS, CHARACTERIZATION, CRYSTAL STRUCTURES AND CORROSION INHIBITION CAPABILITIES OF THE NEW (1*H*-BENZOTRIAZOL-2-YL) METHYL ACETATE AND THEIR ANALOGS

*MITCHELL BACHO [a], FERNANDA OCAYO [b], ALEXANDER TRUJILLO [c], JUAN C. SANTOS [d,e], VANIA ARTIGAS [f], MAURICIO FUENTEALBA [f] AND CARLOS A. ESCOBAR [e,]**

[a]*Facultad de Ciencias Exactas, Departamento de Ciencias Químicas, Laboratorio de Síntesis Orgánica y Organometálica. Universidad Andres Bello, Av. República 330, 8370269, Santiago, Chile.*
[b]*Facultad de Ciencias Exactas, Departamento de Ciencias Químicas, Laboratorio de Corrosión. Universidad Andres Bello, Av. República 330, 8370269, Santiago, Chile.*
[c]*Departamento de Química, Facultad de Ciencias, Universidad de Católica del Norte, Sede Casa Central, Av. Angamos 0610, Antofagasta, Chile.*
[d]*DielecLab, Berlin 791, 8900270, San Miguel, Santiago, Chile.*
[e]*Departamento de Ciencias Biológicas y Químicas, Facultad de Medicina y Ciencia, Universidad San Sebastián, Campus Los Leones, Lota 2465, 7510085, Providencia, Santiago, Chile.*
[f]*Facultad de Ciencias, Instituto de Química, Pontificia Universidad Católica de Valparaíso, Av. Universidad N. 330, 2370000, Curauma, Valparaíso, Chile.*

ABSTRACT

The products of 1*H*-benzotriazole-1-methanol **1** O-acetylation, and their corrosion inhibition capabilities are reported. The O-acetylation of **1** led to the formation of 1-acetyl-1*H*-benzotriazole **4** as the major product and minor quantities of the O-acetylated isomeric acetates **2** and **3**. Molecular structures were determined by NMR Spectroscopy, HRMS, and Single crystal X-ray diffraction. STM D1275-06 test was used to assess the corrosion inhibition capabilities. Compound 1 was the most active inhibitor. Substitution at N2 position is not recommended when looking for inhibition capabilities, the electron attracting capacity and the substituent's size are important for an effective interaction with the copper surface.

Keywords: Benzotriazole, acetylation, corrosion, DFT.

1. INTRODUCTION

The failures in electrical power transformers caused by copper corrosion have their origin in the corrosive sulfur contained in mineral insulating oils used as a refrigerant in power transformers. Sulfur content in insulating oils comes mainly from the sulfur containing antioxidant compounds added not only intending to inhibit the oil aging but also to inhibit the acid formation and prevent crusts deposition on cooper surfaces.[1] In the last fifteen years, dibenzyl disulfide (DBDS) has become one of the most popular sulfur containing antioxidants added to insulating oils.[2] The presence of these kinds of sulfur compounds has been detected in power electrical transformers presenting failures due to corrosion of its copper windings.[3] When an electric power transformer is in-service, the sulfur compounds can corrode the copper metal forming copper sulfide, which modifies the strength of the electric field in the windings and reduces the insulation capacity of the oil, leading to failures in the power equipment. To face this problem, especially in power transformers containing DBDS doped oils, still in-service today, the addition of "passivators" or inhibitors, agents capable to inhibit the interaction between DBDS and metallic copper has been explored.[4,5] In the electrical industry, to avoid copper corrosion when immersed in dielectric mineral oil, benzotriazole (BTAH) derivatives or mixtures of them have been used. Since dielectric oils are mainly composed of hydrocarbons and naphthenic compounds and have a polarity completely different from that of the aqueous medium, a significant decrease in the BTAH solubility has been observed. In this regard, the functionalization of BTAH could improve their solubility in electrical oils, maintaining its properties as an inhibitor of copper corrosion in electrical power transformers, as is the case of the industrial product named Irgamet® 39, a BTAH derivative containing a -CH_2-N-(n-C_8H_{17})$_2$ alkyl group connected at N1 position of the benzotriazole core.[6] In terms of its importance in the electrical industry, the functionalization of BTAH has been a subject of investigation during last decade. In this term, Katritzky[7] developed the use of the N-formylbenzotriazole as an O- and N-formylating agent,[8] but also the use of the N-acylbenzotriazole[9] as an effective acylating reagent. In particular, the synthesis[10–12] and the X-ray molecular structure[13,14] for 1*H*-benzotriazole-1-methanol **1** have been reported previously. For the O-acetylation of **1**, Katritzky used acetic anhydride in acetic acid as solvent[15] to obtain only the (1*H*-benzotriazol-1-yl)methyl acetate **2** with 30% yield. The compound was characterized through traditional spectroscopical techniques but not by Single crystal X-ray diffraction. Its isomer, the (1*H*-benzotriazol-2-yl)methyl acetate **3**, remained unknown.

Based on the previously described antecedents, we describe our attempts to find the elusive (1*H*-benzotriazol-2-yl)methyl acetate **3** by O-acetylation of 1*H*-benzotriazole-1-methanol **1**, the formation of 1-acetyl-1*H*-benzotriazole **4**, as the main reaction product, that can be explained by the mechanism initially proposed by Katritzky.[9] But also, we describe here for the first time the complete XR characterization of the (1*H*-benzotriazol-1-yl)methyl acetate **2**, the synthesis and Single crystal X-ray diffraction of the new (1*H*-benzotriazol-2-yl)methyl acetate **3** and finally, for all the benzotriazole derivates presented in this work, Figure 1, we explored their efficiency as corrosion inhibitors by using the Copper strip corrosion assay.

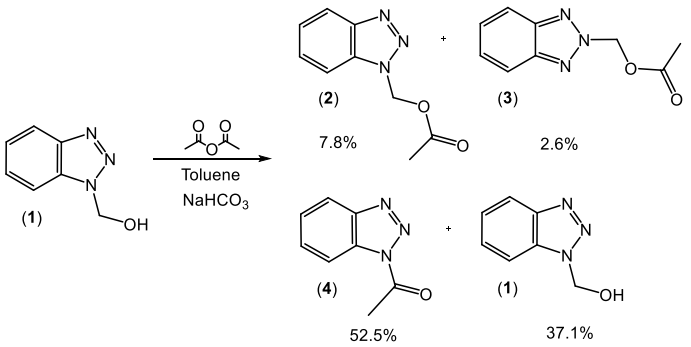

Figure 1. General synthesis conditions for the acetylation of 1*H*-benzotriazole-1-methanol **1**.

2. EXPERIMENTAL

2.1 *General experimental procedures*

All manipulations were carried out at room temperature. The solvents were dried and distilled according to standard procedures. 1*H*-benzotriazole was purchased from Sigma-Aldrich (Saint Louis, USA) and used without further purification. FT-IR spectra were recorded as KBr pellets on a Perkin-Elmer Spectrum Two FT-IR spectrophotometer in the 4000 to 400 cm^{-1} range. The ^1H and ^{13}C NMR spectra were recorded on a Bruker Avance 400 Digital. All NMR spectra are reported in ppm (δ) relative to tetramethylsilane (TMS), used as an internal standard. Coupling constants (J) are reported in Hertz (Hz), and

*Corresponding author email: carlos.escobarza@uss.cl

integrations are reported as the number of protons. The following abbreviations are used to describe peak patterns: s = singlet, d = doublet, t = triplet, m = multiplet, and br = broad. Melting points were determined in open capillaries using a Stuart Scientific SMP3 melting point apparatus (Barloworld Scientific, United Kingdom). HRMS were obtained on a compact QTOF MS + Elute UHPLC with Bruker Compass Data Analysis (Version 4.4) system (Bruker Daltonics Inc., Billerica, MA, USA) using electro-spray ionization.

2.2 *Synthesis*

2.2.1 ***Synthesis of 1H-Benzotriazole-1-methanol 1*****:** 1*H*-benzotriazole-1-methanol **1** was prepared following a previously described procedure.[10]

1*H*-Benzotriazole-1-methanol 1: White solid: yield 65% (3.23 g), mp 149.9-150.4 °C (Lit. = 148-151°C), R_f = 0.05 (1:6 Ethyl acetate: Hexanes). ^{1}H NMR (400 MHz, $CDCl_3$): δ (ppm) 6.10 (2*H*, s, CH_2), 7.38 (1H, t, *J* 7.6 Hz, H_{arom}), 7.52 (1H, t, *J* 7.6 Hz, H_{arom}), 7.69 (1H, d, *J* 8.3 Hz, H_{arom}) 8.04 (1H, d, *J* 8.4 Hz, H_{arom}).

2.2.2 ***Synthesis of (1H-Benzotriazol-1-yl)methyl acetate 2, (1H-benzotriazol-2-yl)methyl acetate 3 and 1-acetyl-1H-benzotriazole 4*****:** Compound **1** (0.6 g, 4 mmol) was dissolved in toluene (24 mL) and solid grounded sodium bicarbonate (0.7 g, 8 mmol) was added. Then, acetic anhydride (2.0 g, 20 mmol) was added to the reaction mixture and was allowed to react for two hours. The course of the reaction was followed by TLC (Ethyl acetate: Hexanes = 1:1 v/v). Then, the reaction mixture was filtered, and toluene was evaporated under vacuum to obtain a mixture of compounds (**1**, **2**, **3** and **4**), that were purified by column chromatography (silica gel 60, Ethyl acetate: Hexane = 1:6 v/v) to give the title compounds **2-4**.

(1*H*-Benzotriazol-1-yl)methyl acetate 2: White solid; Yield 7.8 % (0.06 g), mp 58.1- 60.0 °C, R_f = 0.16 (1:6 Ethyl acetate:Hexanes). Slow evaporation from deuterated chloroform produced Colorless crystals. IR (KBr) n/cm^{-1}: 1756 (C=O), 1366 (-CO-CH_3). ^{1}H NMR (400 MHz, $CDCl_3$): δ (ppm) 2.11 (3H, s, CH_3), 6.59 (2H, s, CH_2), 7.40 (1H, td, *J* 1.0, 8.2 , 7.0 Hz, H_5), 7.54 (1H, td, *J* 1.0, 8.2, 7.0 Hz, H_6), 7.75 (1H, td, *J* 1.0, 1.0, 8.4 Hz, H_7), 8.06 (1H, td, *J* 1.0, 1.0, 8.4 Hz, H_4). ^{13}C NMR (100 MHz, $CDCl_3$): δ (ppm) 20.6, 67.8, 110.0, 120.0, 124.6, 128.5, 132.9, 146.2, 170.1. HRMS (EI) *m/z*, Calculated for $C_9H_9N_3O_2Na$ $[M+Na]^+$: 214.0587, found: 214.0589.

(1*H*-Benzotriazol-2-yl)methyl acetate 3: White solid, yield 2.6 % (0.02 g); mp 68.9- 69.7 °C, R_f = 0.28 (1:6 Ethyl acetate:Hexanes). Colorless crystals were obtained by recrystallization using ethanol. IR (KBr) n/cm^{-1}: 1746 (C=O), 1373(-CO-CH_3). ^{1}H NMR (400 MHz, $CDCl_3$): δ (ppm) 2.16 (3H, s, CH_3), 6.57 (2H, s, CH_2), 7.43 (2H, dd, *J* 6.6, 3.1 Hz, H_5, H_6), 7.90 (2H, dd, *J* 6.6, 2.9 Hz, H_1, H_7). ^{13}C NMR (100 MHz, $CDCl_3$): δ (ppm) 20.6, 75.3, 118.6, 127.5, 145.1, 169.2. HRMS (EI) *m/z*, Calculated for $C_9H_{10}N_3O_2$ $[M+H]^+$: 192.0768, found; 192.0769.

1-acetyl-1*H*-benzotriazole 4: White solid, Yield 52.5 % (0.34 g); mp 47.9-48.3 °C, R_f = 0.47 (1:6 Ethyl acetate: Hexanes). Colorless crystals were obtained by recrystallization using ethanol. IR (KBr) n/cm^{-1}: 1735 (C=O), 1372 (-CO-CH_3). ^{1}H NMR (400 MHz, $CDCl_3$): δ (ppm) 2.99 (3H, s, CH_3), 7.49 (1H, td, *J* 8.2, 7.1, 1.1 Hz, H_{arom}), 7.64 (1H, td, *J* 8.2, 7.1, 1.1 Hz, H_{arom}), 8.10 (1H, dt, *J* 8.1, 1.8, 1.0 Hz, H_7), 8.27 (1H, dt, *J* 8.3, 1.9, 1.0 Hz, H_4). ^{13}C NMR (100 MHz, $CDCl_3$): δ (ppm) 22.2, 113.4, 119.1, 125.1, 129.4, 130.0, 145.3, 168.6.

2.3 *X-ray Crystal Structure Determination for Compounds 2 and 3*

Crystals of compounds **2** and **3** suitable for Single crystal X-ray diffraction were obtained as described above. The single crystals were mounted using MiTeGen MicroMounts. Table S3 to S5 contain the experimental and crystallographic data, selected bond distances and the intermolecular interactions for all studied compounds. Complete details of the crystals, X-ray data collection, and structure solution are provided in the supplementary data. Intensity data were collected at room temperature for compounds **2** and **3** on a Bruker D8 QUEST diffractometer equipped with a bidimensional CMOS Photon100 detector using graphite monochromated Mo-Kα radiation. The diffraction frames were integrated using the APEX3[16] package. The solution and refinement for the isolated compounds were carried out with Olex2.[17] All structures were solved by direct methods and refined with the SHELXL[18] refinement package using least squares minimization. The complete structures were refined using the full matrix least squares procedure on the reflection intensities (F2). All non-hydrogens were refined with anisotropic displacement coefficients, and all hydrogen atoms were placed in idealized locations. For compound **2**, the oxygen atoms at carbonyl's ester group were modeled, at room temperature, with fixed occupancies of 0.61/0.39. The restraints SADI at 0.001 (O2 and O2A) were used.

2.4 *Theoretical calculations*

All geometry optimizations reported in this work were studied in the framework of Density Functional Theory. A B3LYP[19,20] exchange–correlation functional with def2TZVP[21] basis set were used as level of calculation, and finally, the nature of the stationary points and the zero-point energy corrections were examined by calculating the Hessian matrix at the same level. To understand the stability, the polarizability was calculated with the aim to explore correlations between energy and the minimum polarizability principles, which states that any system evolves naturally toward a state of minimum polarizability.[22] Solvent effect for simulating toluene has been incorporated through the polarizable continuum model (PCM). All calculations were made using Gaussian09[23] package of programs.

2.5 *Corrosion assay in dielectric oil*

To assess the inhibition capabilities of the benzotriazole analogs prepared, an inhibition assay was conducted. The procedure for evaluating these capabilities is described in the Standard Test Method for Corrosive Sulfur in electrical oils, ASTM D1275-06. For this reason, the ASTM D1275 B and D130/IP154 methodologies were implemented in our laboratory. Typically, Corrosion assays were performed as follows: First, a commercial dielectric oil showing any corrosive capability was selected to perform the inhibition assay. Then, typically, a stock solution of this oil containing 400 mg of added DBDS in 2 L oil was prepared. Then, 250 mL aliquots of this solution containing 200 ppm of DBDS were taken and placed in a 250 mL Duran glass bottle. Then different amounts of the Benzotriazole compound to be tested were added to reach 1, 3 and 5 ppm benzotriazole/250 mL oil. At this point, an L-shaped folded polished copper strip (5 cm long x 1.3 cm wide), washed with acetone, and dried at room temperature, was submerged in the DBDS/benzotriazole containing solution, then, to eliminate the dissolved air, the copper strip/DBDS/benzotriazole containing oil, was bubbled for 5 min with nitrogen, and rapidly sealed with a Duran screw cap GL45. Two replicates for each benzotriazole tested were prepared, and then, simultaneously exposed to 150º C for 72 hours in an oven. At the end of this time, the flasks were allowed to cool down, and then, the copper strips were removed from the oil, and their coloration was compared with the D130 ASTM copper strip corrosion color scale, to assess the corrosion extent, produced by the DBDS over the copper strip. A control assay was included in all experiments. The control contained the same setup previously mentioned, but without inhibitor, and was used to assess the corrosion capability of the solution.

3. RESULTS AND DISCUSSION

3.1 *Chemistry*

1*H*-benzotriazole-1-methanol **1** was obtained as a crystalline solid, in accordance with the previously reported data[13,14] (Supplementary material (SM), Figure S1, Table S1). The ^{1}H-NMR spectra of **1** in deuterochloroform showed the presence of a tautomeric mixture of compounds **1** and **1a** (Figure 2) in a ratio of 2:1, respectively (SM, Figure S1). This tautomeric equilibrium was explained previously by Tomas *et al*. and Figure 2 shows the tautomeric rearrangement occurring in benzotriazoles.[24] To perform the O-acetylation a previously reported methodology was selected, using acetic anhydride as the acylating agent, in toluene catalyzed by sodium bicarbonate.[25] As previously mentioned, Katritzky performed the O-acetylation of **1** with 30% yield using acetic anhydride but in acetic acid as solvent[26] to obtain only the (1*H*-benzotriazol-1-yl)methyl acetate **2**. In our case, after column chromatography, compound **2** was obtained with a 7.8% yield, but also we were able to isolate for the first time, its isomeric product the (1*H*-benzotriazol-2-yl)methyl acetate **3**, with 2.6% yield. Also, the 1-acetylbenzotriazole **4** with 52.5% yield and 37.1% of **1,** formed as byproduct, were obtained, Figure 1.

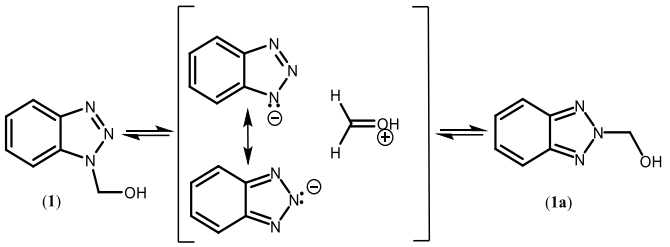

Figure 2. Tautomerization mechanism from **1** to 1*H*-benzotriazole-2-methanol **1a**.

(1*H*-Benzotriazole-1-yl)methyl acetate **2** was isolated as colorless crystals (mp. = 58.1-60 °C, deuterated chloroform), and their molecular structure was determined by one dimensional NMR spectroscopy and single-crystal diffraction. ^{1}H NMR spectra showed a similar pattern of signals to 1*H*-benzotriazole core in the aromatic zone (SM, Figure S2 and S3). The presence of four signals, associated with the aromatic hydrogens present in H4, H5, H6, and H7, were found at d_H 7.42 ppm (*ddd*, 1H, J=8.2, 7.0, 1.0, H5), 7.56 ppm (*ddd*, 1H, J=8.3,7.1, 1.0, H6), 7.77 ppm (*dt*, 1H, J=8.4, 0.9, H7), and 8.08 ppm (*dt*, 1H, J=8.4, 0.9, H4). Likewise, it is possible to observe a signal associated with the methylene group at d_H 6.59 ppm (s, 2H) and the methyl fragment at d_H 2.11 ppm (s, 3H). IR bands at 1756 (C=O) and 1366 (-CO-CH_3) cm^{-1} supports the O-acetylation of the 1*H*-benzotriazole-1-methanol. The ^{13}C NMR analysis showed the presence of nine carbons associated with the 1*H*-benzotriazole core and the methyl acetate fragment present in **2**. The signals at d_C 170.02 ppm were assigned to the carbonyl group and d_C 20.56 ppm to the methyl group of the ester moiety (SM, Figure S4). Moreover, mass spectrometry of this compound shows a $[M+Na]^+$ ion peak at m/z 214.0589, (Figure S11), which is consistent with the formula $C_9H_9N_3O_2Na$. These data confirms the acetylation of the 1*H*-benzotriazole-1-methanol to (1*H*-benzotriazole-1-yl)methyl acetate **2**.

(1*H*-Benzotriazole-2-yl)methyl acetate **3** was isolated as colorless crystals (mp. = 68.9-69.7 °C, methylene dichloride), and their molecular structure was determined by one dimensional NMR spectroscopy and single-crystal X-ray diffraction. For compound **3** was possible to observe four signals in the ^{1}H NMR spectra. The decrease in the number of observed signals is associated with the symmetry of this compound (SM, Figure S5 and S6). The set of signals at d_H 7.43 ppm (*m*, 2H, H5 and H6) and d_H 7.90 ppm (*m*, 2H, H4-H7) are consistent with the chemical shift for 1*H*-benzotriazole core in 1*H*-benzotriazole-2-methanol.[27] Also, the presence of methyl fragment at d_H 2.16 (s, 3H, CH_3) confirms the acetylation, and are consistent with the bands observed in IR spectra at 1746 (C=O), 1373(-CO-CH_3) cm^{-1}. In parallel, the ^{13}C NMR analysis showed the characteristic chemical shift for the 1*H*-benzotriazole fragment (SM, Figure S7). Additionally, the presence of the signal at d_C 169.24 ppm for the carbonyl group and at d_C 20.58 ppm for the methyl fragment confirms the acylation. mass spectrometry of this compound shows a $[M+H]^+$ ion peak at m/z 192.0768, (Figure S12), which is consistent with the formula $C_9H_{10}N_3O_2$. Previously information confirmed the acylation of 1*H*-benzotriazole-2-methanol to (1*H*-benzotriazole- 2-yl) methyl acetate.

In the same way, 1-acetylbenzotriazole **4** was isolated as colorless needles (mp. = 47.9-48.3 °C, n-pentane), and their molecular structure was also determined by Single crystal X-ray diffraction. The NMR spectra and the structural parameters are found in the supplementary data in Figures S8-S10, S16 and Tables S6-S8.

To explain the presence of each product in the reaction mixture, the direct O-acylation of **1** and its isomer **1a**, formed via tautomeric rearrangement, using acetic anhydride and sodium bicarbonate take place, producing the formation of the O-acetylated products **2** and **3**, respectively but also acetic acid as a byproduct (Figure 2). As described previously by Katritzky[26], the treatment of compound **1** in the presence of acetic acid and acetic anhydride produced the N-acylated product **4**. This proposed mechanism could explain the formation of **4** in our case: The acetic acid required was produced in the reaction mixture as a byproduct of the O-acylation of **1** and **1a** (Figure 2), then, the so produced acetic acid in presence of excess acetic anhydride (used in excess as solvent) could have reacted with compound **1** to form the compound **4** as described previously by Katritzky[26] and could also explain the recovery of "unreacted" **1**, the proposed mechanism is summarized in Figure 3.

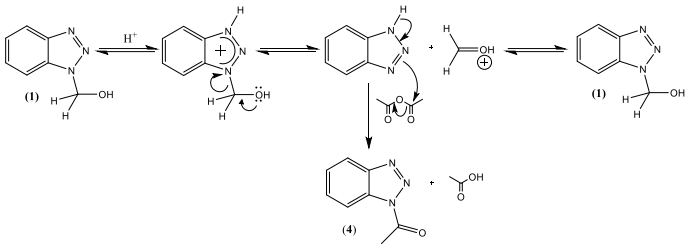

Figure 3. Mechanism proposed to explain the formation of **4** and the recovery of "unreacted" **1**, based in a previous mechanism proposed by Katritzky.

3.2 *X-Ray crystallographic analysis*

ORTEP drawings of compounds **2** and **3** along with the atom numbering scheme, are shown in Figure 4. Tables S3-S5 shows the crystal data collection and structure parameters for compounds entitled.

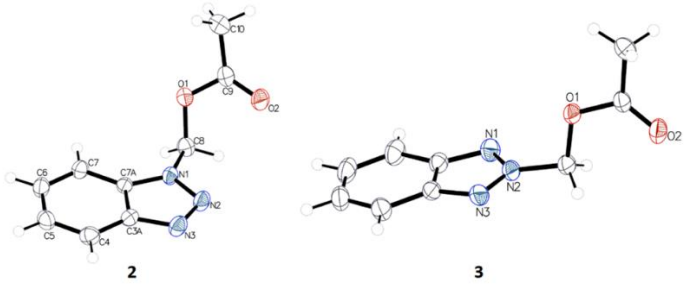

Figure 4. ORTEP diagram for (1*H*-Benzotriazol-1-yl)methyl acetate **2** and (1*H*-benzotriazol-2-yl)methyl acetate **3** with the heteroatom numbering scheme. Thermal ellipsoids are drawn at 30% probability.

The compounds crystallized in the monoclinic space group $P2_1/c$, observing the presence of one molecular entity in the asymmetric unit, Figure 4. Table S8 exhibits a selection of bond distances and angles. For compounds **2** and **3**, the metrical parameters of the benzotriazole fragment and methyl acetate fragment are like those reported by Xu *et al*.[28]

In addition, for compound **2** the plane formed by the benzotriazole core and the substituent located at N1 showed to be almost perpendicular, with a torsion angle of 104.2(16)°. In the same way, for compound **3** the plane formed by the benzotriazole core and the substituent located at N2 showed to be almost perpendicular, with a torsion angle of 83.53°. In contrast with the report by Xu *et al.*,[28] this plane exhibits a torsion angle of 119.73°, losing the perpendicular character, due to the presence of the phenyl ring, which gives larger electronic delocalization to the structure.

Finally, the crystallographic intermolecular interactions analysis showed for benzotriazole **2** a hydrogen bond C(8)-H(8A)···O2 by a twofold screw axis (Figure S14 and Table S4), and is in accordance with the data reported in the literature for this H-bond interaction.[29] Also, a π–π interaction among the benzene rings with an angle of 8.869(10)°, a centroid-centroid distance of 3.673(10) Å and a shift distance of 0.992(10) Å, were measured.

In contrast with benzotriazole **2**, crystallographic intermolecular interactions analysis for **3** showed only a set hydrogen bonds of the type C-H···X (X=N, O), C4-H4···O2 and C(8)-H(8B)···N3 by an inversion center, C(6)-H(6)···O2 by a *c*-glide plane and C(10)-H(10C)···O2 by a twofold screw axis (Figure S15).

3.3 *DFT calculations*

The results obtained through the theoretical calculations are summarized in Table 1. Our results show that in all cases, the most stable structures are the N1-substituted compounds and that they have smaller polarizability and lower energy than their N2-substituted isomers. A small energy difference between compounds **1** and **1a** was found, but also between compounds **2** and **3**. This small energy difference between the N1 and N2-isomers could explain the presence of these products in the reaction mixture. The energy difference increases for the

N1- and N2-acetylated compounds, which could explain the exclusive presence of compound **4** and not their N2-Acetylated isomer. These results of stability agree with the increases in energy difference between isomers and are supported by the minimum polarizability principle.

Table 1. Relative Energy of N1 vs N2 substituted isomers (ΔE[a], including the ZPE correction) and polarizability for the studied compounds.

	Gas		Toluene	
Compound	**α**	**ΔE**	**α**	**ΔE**
1	103.6	-0.3	119.6	-1.0
1a	106.5		122.9	
2	130.63	-0.6	149.0	-1.3
3	135.05		153.7	
4	115.1	-5.9	133.1	-5.6
4'[b]	120.1		139.1	

[a]ΔE=EN1-EN2; Where EN1 and EN2 correspond to the Energy of N1 and N2 substituted compounds, respectively.

[b]This refers to 1*H*-benzotriazole-2-methanol, compound not isolated/prepared.

3.4 *Corrosion assay*

Among the studied compounds, the one that showed the best corrosion inhibition capacity was compound **1**. The compound that did not present any inhibitory capacity was compound **2**. While compound **3** showed inhibition at 5 ppm and compound **4** at 3 and 5 ppm, respectively. These results suggest that the inhibitory capacity in the different systems seems to be affected by two factors i) the substituent's electron attracting capacity and ii) the substituent's size. While in compound **1**, a small sized electron donor group is found, meanwhile in the other systems large electron attracting groups are located. It seems that the electron attracting groups decrease the electronic density on the triazole ring, reducing its ability to interact with the copper metal surface. Additionally, the steric hindrance imposed by the large substituents also reduces its ability to interact with the metal surface. In contrast, a small sized electron donor group has little steric hindrance and increases the electronic density on the triazole ring, promoting its ability to interact with the copper metal surface. Table 2 summarizes the corrosion level observed in copper strips according to the ASTM test method D130/IP 154. Images of some copper probes after the corrosive sulfur test are reported in Table S9.

Finally, in our previous theoretical work[30] it was possible to determine the role of benzotriazoles as copper surface's passivators and their adsorption competitivity against DBDS. We found that the complexes were formed by electron transfer from the surface to the adsorbate and the most stable one, that with higher adsorption energy, corresponds to those with lower geometrical deformation. In the case of this study, results found for compounds **1** and **1a**, agree with those previous results, since their size ensures the minimal steric hindrance (the least deformation) and the greatest availability to interact perpendicularly with the copper surface.

Table 2: Copper strip corrosion assay, for compound **1** to **4**.

Concentration	**1**	**2**	**3**	**4**
5 ppm	1b/ST	4b/CO	1b/ST	1b/ST
3 ppm	1b/ST	4b/CO	3a-3b/DT	1b/ST
1 ppm	1b/ST	4b/CO	3b-4a/DT-CO	4b-4c/CO

ST =Slight tarnish; CO = Corrosion; DT = Dark tarnish; The control sample containing 200 ppm of DBDS, without inhibitor, always showed corrosion at 4c level.

CONCLUSIONS

In summary, we have reported here the synthesis, isolation and single crystal X-Ray characterization of the (1*H*-benzotriazol-2-yl)methyl acetate **3** and the X-ray molecular structure characterization of its isomer, the (1*H*-benzotriazol-1-yl)methyl acetate **2**, both for the first time. DFT calculations showed that in all cases, the most stable structures are the N1-substituted benzotriazoles and that they have smaller polarizability and lower energy than their N2-substituted isomers. Interestingly, the small energy difference for the precursor compound **1** and **1a** and their methyl acetates **2** and **3**, explain the presence of all of them in the reaction mixture. The O-acetylation of **1** and its tautomer **1a** via acetic anhydride and sodium bicarbonate in toluene produced acetate **2** and its isomer **3**, but also acetic acid as a byproduct, thus promoting a reaction, that was initially described by Katritzky, were the precursor **1** is protonated to yield 1-acetylbenzotriazole **4**, the reaction's main product. The corrosion inhibition capacity of the obtained compounds was analyzed to assess the role of the substituted benzotriazoles, prepared in this work as copper surface's passivators and their adsorption competitiveness against DBDS. The better results were obtained with compound **1**, reaching an effectivity of 1:200 (passivator: corrosive agent), higher than the other benzotriazole evaluated in this work. Although, the acetylation did not generate better inhibitory capabilities, it was possible to identify that the hydroxyl group must not be substituted to get better corrosion capabilities and that the N2 position is not the best to locate substituents when looking for better corrosion inhibition. These results agree with both, the electron attracting capacity and the substituent's size, which enable an effective interaction with the copper surface.

ACKNOWLEDGMENTS.

The authors gratefully acknowledge the financial support from UNAB (grant N° DI-16-19/R), to the FONDECYT ANID POSTDOCTORAL grant No. 3220756, to the Fondo de Equipamiento Científico y Tecnológico FONDEQUIP, grant No. EQM120095 (Single crystal X-ray diffractometer) and the EQM170172 (Compact QTOF MS).

SUPPLEMENTARY INFORMATION

The structures of Compounds 2 and 3 in this article have been deposited to the Cambridge Crystallographic Data Centre (CCDC) under the accession number 1970138 and 1970139 (www.ccdc.cam.uk/data_request/cif).

REFERENCES

1. Maina, R.; Tumiatti, V.; Pompili, M.; Bartnikas, R.; *IEEE Transactions on Dielectrics and Electrical Insulation*, **2009**, *16*, 1655. [https://doi.org/10.1109/TDEI.2009.5361586]
2. Arvidsson, L.; *IEEE International Symposium on Electrical Insulation*, **2010**, 4. [https://doi.org/10.1109/ELINSL.2010.5549741]
3. Bruzzoniti, M. C.; Sarzanini, C.; Rivoira, L.; Tumiatti, V.; Maina, R.; J Sep Sci, **2016**, 39, 2955. [https://doi.org/10.1002/jssc.201600311]
4. Samarasinghe, S.; Ma, H.; Ekanayake, C.; Martin, D.; Saha, T.; *IEEE Transactions on Dielectrics and Electrical Insulation*, **2020**, *27*, 1761. [https://doi.org/10.1109/TDEI.2020.008996]
5. Krishnarmoorthy, P. R.; Vijayakumari, S.; Krishnaswamy, K. R.; Thomas, P.; *Proceedings of the 3rd International Conference on Properties and Applications of Dielectric Materials*, **1991**, 732. [https://doi.org/10.1109/ICPADM.1991.172169]
6. Martins, M. A. G.; Gomes, A. R.; *IEEE Electrical Insulation Magazine*, **2010**, *26*, 27. [https://doi.org/10.1109/MEI.2010.5511186]
7. Katritzky, A. R.; Rachwal, S.; *Chem Rev*, **2011**, *111*, 7063. [https://doi.org/10.1021/cr200031r] http://www.ncbi.nlm.nih.gov/pubmed/19799386
8. Katritzky, A. R.; Chang, H.-X.; Yang, B.; *Synthesis* (Stuttg) **1995**, *1995*, 503. [https://doi.org/10.1055/s-1995-3959]
9. Katritzky, A. R.; He, H.-Y.; Suzuki, K.; *J Org Chem* **2000**, *65*, 8210. [https://doi.org/10.1021/jo000792f]
10. Burckhalter, J. H.; Stephens, V. C.; Hall, L. A. R.; *J Am Chem Soc* **1952**, *74*, 3868. [https://doi.org/10.1021/ja01135a044]
11. Katritzky, A. R.; Yannakopoulou, K.; Lue, P.; Rasala, D.; Urogdi, L. ;J *Chem Soc Perkin 1* **1989**, *2*, 225
12. Hong, Y. S.; Kim, H. M.; Kirn, H. S.; Park, Y. T.; *Bull Korean Chem Soc* **1999**, *20*, 1524.
13. Liu, Q.-X.; Xu, F.-B.; Li, Q.-S.; Zeng, X.-S.; Leng, X.-B.; Zhang, Z.-Z.; *Chin J Chem* **2010**, *20*, 878. [https://doi.org/10.1002/cjoc.20020200914]
14. Alkorta, I.; Elguero, J.; Jagerovic, N.; Fruchier, A.; Yap, G. P. A.; *J Heterocycl Chem* **2004**, *41*, 285. [https://doi.org/10.1002/jhet.5570410223]
15. Katritzky, A. R.; He, H.-Y.; Suzuki, K.; *J Org Chem* **2000**, *65*, 8210. [https://doi.org/10.1021/jo000792f]
16. Bruker, M.; *Apex3 and SADABS.* **2016,** Bruker AXS Inc., Wisconsin, USA.
17. Dolomanov, O. V.; Bourhis, L. J.; Gildea, R. J.; Howard, J. A. K.; Puschmann, H.; *J Appl Crystallogr* **2009**, *42*, 339. [https://doi.org/10.1107/S0021889808042726]

18. Sheldrick, G. M.; *Acta Crystallogr A* **2008**, *64*, 112. [https://doi.org/10.1107/S0108767307043930]
19. Becke, A. D.; *Phys Rev A* (Coll Park) **1988**, *38*, 3098. [https://doi.org/10.1063/1.1749835]
20. Lee, C.; Yang, W.; Parr, R. G.; *Phys Rev B* **1988**, *37*, 785. [https://doi.org/10.1103/PhysRevB.37.785]
21. Weigend, F.; Ahlrichs, R.; *Physical Chemistry Chemical Physics* **2005**, *7*, 3297. [https://doi.org/10.1039/b508541a]
22. Chattaraj, P. K.; Sengupta, S.; *J Phys Chem* **1996**, *100*, 16126. [https://doi.org/10.1021/jp961096f]
23. M. J. Frisch; Pittsburgh, PA, **2009**.
24. Tomas, F.; Abboud, J. L. M.; Laynez, J.; Notario, R.; Santos, L.; Nilsson, S. O.; Catalan, J.; Claramunt, R. M.; Elguero, J.; *J Am Chem Soc* **1989**, *111*, 7348. [https://doi.org/10.1021/ja00201a011]
25. Lugemwa, F.; Shaikh, K.; Hochstedt, E.; *Catalysts* **2013**, *3*, 954. [https://doi.org/10.3390/catal3040954]
26. Katritzky, A. R.; Rachwal, S.; Rachwal, B.; *J. Chem. Soc., Perkin Trans. 1* **1987**, 791. [https://doi.org/10.1039/P19870000791]
27. Katritzky, A. R.; Perumal, S.; Savage, G. P.; *Journal of the Chemical Society, Perkin Transactions 2* **1990**, 921. [https://doi.org/10.1039/p29900000921]
28. Xu, S.; Shen, Y.; *Acta Crystallogr Sect E Struct Rep Online* **2012**, *68*, 1066. [https://doi.org/10.1107/S1600536812010252]
29. Jeffrey, G. A.; *Crystallogr Rev* **2003**, *9*, 135. [https://doi.org/10.1080/08893110310001621754]
30. Saavedra-Torres, M.; Escobar, C. A.; Ocayo, F.; Tielens, F.; Santos, J. C.; *Chem Phys Lett* **2017**, *689*, 128. [https://doi.org/10.1016/j.cplett.2017.09.067]